Affine Formation Obstacle Avoidance Control of Unmanned Aerial Vehicles with Prescribed Convergence Time

Jiacheng Li[1], YangWang Fang[1*], Shuaiqi Huangfu[1], Mengjie Zeng[2], Guangyu Yang[3], and Tianbo Deng[4]

[1] Unmanned System Research Institute, Northwestern Polytechnical University, Xian, China
ywfang@nwpu.edu.cn,
[2] College of Energy and Power Engineering, Nanjing University of Aeronautics and Astronautics, Nanjing, China
[3] School of Marine Science and Technology, Northwestern Polytechnical University, Xian, China
[4] School of Astronautics, Northwestern Polytechnical University, Xian, China

Abstract. A novel affine formation obstacle avoidance control method with prescribed convergence time for Unmanned Aerial Vehicles (UAVs) is presented in this paper. For engineering realization, the conventional stress matrix of the affine formation is divided into the Laplace matrix for communication and the variable weight matrix for formation control. Then, the obstacle avoidance item with repulsion is introduced into the control algorithm of the formation, which can ensure that no collisions occur among the UAVs during their flying process. Furthermore, a time-varying scaling function is proposed to achieve the formation form the desired shape within a prescribed time. Finally, simulation results verify the correctness and effectiveness of the proposed affine formation control method.

Keywords: Affine formation, Obstacle avoidance, UAVs, Prescribed Convergence Time

1 Introduction

Recently, there has been tremendous interest in developing the control algorithm for UAVs formation to avoid obstacles [1]. Many methods were applied to obstacle avoidance, such as Model Predictive Control (MPC), Artificial Potential Field method (APF), and so on [2]. However, these approaches are only valid within a certain range, but are no longer effective when the obstacles are too large. To solve this problem, the formation shape and maneuver control was studied [3].

A series of affine formation control methods have been developed to achieve formation transformation [4–8]. Zhao proposed the leader-follower strategy to achieve the formation maneuver control based on stress matrices in Ref. [4], which not only can form the desire formation, but also can track any time-varying affine transformation. In recent years, the distributed affine formation control algorithms have been proposed, which face second-order multi-agent system [5,6], high-order multi-agent system [7], and Fixed-Wing UAVs [8], respectively. It is worth to mention that therein these distributed control schemes do all have high feasibility on formation transformation.

Furthermore, convergence within a specific time is necessary for formation control because many practical formation tasks have timing requirements. In this way, the affine formation control problem for multi-agent systems with prescribed convergence time was investigated in Ref. [9], which achieves better performance and robustness for the formation system. Inspired by the collective behaviors such as bird immigration, Ref. [10] proposed a finite-time bearing-based control laws for acyclic leader-follower formation, which improves formation efficiency greatly.

To achieve the two control objectives of formation obstacle avoidance and predetermined time convergence [11] in the same time, a novel control algorithm is designed in this paper. The main contributions of this work include three aspects. Firstly, an affine formation maneuver algorithm is designed for obstacle avoidance, in which the stress matrix is improved to make the work more in line with engineering practice. Secondly, the repulsion term based on the potential field is constructed to ensure every UAV collision-free flight. Finally, the convergence time of UAVs formation system can be prescribed in advanced.

2 Problem statement and preliminaries

In this section, some basic and useful concepts about UAVs formation are presented.

2.1 Graph description

An undirected graph $G = (V, \varepsilon)$ is used to describe the interaction among UAVs, which consists of a node set $V = \{1, 2, ..., n\}$ and an edge set $\varepsilon \subseteq V \times V$. The edge $(i, j) \in \varepsilon, i \neq j$ means that the ith UAV can receive information from the jth UAV. In this paper, assume that the underlying graphs are undirected and we have $(i, j) \in \varepsilon \Leftrightarrow (j, i) \in \varepsilon$. The formation is defined as $(G, \boldsymbol{p})$ which is a configuration $\boldsymbol{p}$ combing with a communication graph G.

2.2 Basic notations of affine formation

First of all, we give some notations: α_i represents the ith UAV in the formation; $\boldsymbol{q}_i$ and $\boldsymbol{p}_i$ represent the position and speed of the ith UAV, respectively; $\boldsymbol{u}_i$ is the control input of ith UAV; $\boldsymbol{L}_o$ denotes the safe distance between UAV and obstacle; n, n_l, n_f represent the number of the UAVs, the leaders, and the followers in the formation, respectively. The symbol $\otimes$ denotes the Kronecker product; the symbol $\odot$ is the Hadamard Product; the symbol $\|\|$ denotes the 2-norm of a vector.

Consider a leaders-followers structure formation, the first n_l UAVs are selected as leaders and the other $n_f = n - n_l$ are followers. At this time, the formation positions of n_l leaders are

$$\boldsymbol{q}_l = \left[(\boldsymbol{q}_1)^T, (\boldsymbol{q}_2)^T, \cdots, (\boldsymbol{q}_{n_l})^T \right]^T \tag{1}$$

And the positions of the followers can be expressed as

$$\boldsymbol{q}_f = \left[(\boldsymbol{q}_{n_l+1})^T, (\boldsymbol{q}_{n_l+2})^T, \cdots, (\boldsymbol{q}_n)^T \right]^T \tag{2}$$

In this way, the formation can be described as

$$\boldsymbol{q} = \left[(\boldsymbol{q}_l)^T, (\boldsymbol{q}_f)^T \right]^T \tag{3}$$

Besides, we denote the constant configuration in Eq. (4) as a nominal configuration and the nominal formation can be defined as $(G, \boldsymbol{r})$.

$$\boldsymbol{r} = \left[(\boldsymbol{r}_l)^T, (\boldsymbol{r}_f)^T \right]^T \tag{4}$$

Then, the target formation with maneuver can be expressed as

$$\boldsymbol{q}^*(t) = \left[\boldsymbol{I}_n \otimes \bar{\boldsymbol{A}}(t) \right] \boldsymbol{r} + \mathbf{1}_n \otimes \bar{\boldsymbol{b}}(t) \tag{5}$$

where, $\mathbf{1}_n$ is the n-dimensional column vector of ones; $\bar{\boldsymbol{A}}(t) \in \mathbb{R}^{n \times n}$ and $\bar{\boldsymbol{b}}(t) \in \mathbb{R}^{n \times n}$ are continuous with respect to t, which are used to realize affine transformation of the nominal configuration $\boldsymbol{r}$.

To realize the formation transformation, a stress term is set between UAV α_i and α_j , which satisfies

$$\sum_{j \in N_i} w_{ij} (\boldsymbol{q}_j - \boldsymbol{q}_i) = 0 \tag{6}$$

When $w_{ij} > 0$, there is an attractive force between UAV α_i and α_j; when $w_{ij} < 0$, a repulsive force is set between α_i and α_j. Then, Eq. (6) can be written in a matrix form as

$$(\boldsymbol{\Omega} \otimes \boldsymbol{I}_2)\, \boldsymbol{q} = 0 \tag{7}$$

where $\boldsymbol{\Omega}$ is a stress matrix, which can be defined as

$$\Omega_{ij} = \begin{cases} -w_{ij} & (i \neq j, j \in N_i) \\ 0 & (i \neq j, j \notin N_i) \\ \sum\limits_{j \in N_i} w_{ij} & (i = j) \end{cases} \tag{8}$$

Based on the leaders-followers network, Eq. (7) can be written in the form of a block matrix as

$$\bar{\boldsymbol{\Omega}} = \begin{bmatrix} \boldsymbol{\Omega}_{ll} & \boldsymbol{\Omega}_{lf} \\ \boldsymbol{\Omega}_{fl} & \boldsymbol{\Omega}_{ff} \end{bmatrix} \otimes \boldsymbol{I}_d = \begin{bmatrix} \bar{\boldsymbol{\Omega}}_{ll} & \bar{\boldsymbol{\Omega}}_{lf} \\ \bar{\boldsymbol{\Omega}}_{fl} & \bar{\boldsymbol{\Omega}}_{ff} \end{bmatrix} \tag{9}$$

where, $\bar{\boldsymbol{\Omega}}_{ll} \in \mathbb{R}^{2n_l \times 2n_l}$; $\bar{\boldsymbol{\Omega}}_{lf} \in \mathbb{R}^{2n_l \times 2n_f}$; $\bar{\boldsymbol{\Omega}}_{ff} \in \mathbb{R}^{2n_f \times 2n_f}$ and $\bar{\boldsymbol{\Omega}}_{lf}^T = \bar{\boldsymbol{\Omega}}_{fl}$. According to the Theorem 2 in Ref. [4], $\bar{\boldsymbol{\Omega}}_{ff}$ is nonsingular. Here, the stress matrix can be understood as the control coefficient matrix, which is used to represent the magnitude of the attractive and repulsive forces.

At the same time, the Laplacian communication matrix is defined as follows

$$\bar{\boldsymbol{L}} = \begin{bmatrix} \boldsymbol{L}_{ll} & \boldsymbol{L}_{lf} \\ \boldsymbol{L}_{fl} & \boldsymbol{L}_{ff} \end{bmatrix} \otimes \boldsymbol{I}_d = \begin{bmatrix} \bar{\boldsymbol{L}}_{ll} & \bar{\boldsymbol{L}}_{lf} \\ \bar{\boldsymbol{L}}_{fl} & \bar{\boldsymbol{L}}_{ff} \end{bmatrix} \tag{10}$$

where, $\bar{\boldsymbol{L}}_{fl} \in \mathbb{R}^{2n_f \times 2n_l}$ represents the interaction topology between the leaders and the followers; $\bar{\boldsymbol{L}}_{ll} \in \mathbb{R}^{2n_l \times 2n_l}$ and $\bar{\boldsymbol{L}}_{ff} \in \mathbb{R}^{2n_f \times 2n_f}$ are the interaction topology among the leaders and followers, respectively.

To make better use of affine transformation, several conjectures and definitions are given in the following.

Definition 1. *The nominal formation $(G, \boldsymbol{r})$ is affinely localizable by the leaders if for any $\boldsymbol{p} = \left[\boldsymbol{p}_l^T, \boldsymbol{p}_f^T\right]^T \in \boldsymbol{A}(\boldsymbol{r})$, then $\boldsymbol{p}_f$ can be determined uniquely by $\boldsymbol{p}_l$.*

Conjecture 1. Assume that there are $d+1$ leaders which affinely span $\mathbb{R}^d$ in the nominal formation.

Conjecture 2. Assume that the nominal formation $(G, \boldsymbol{r})$ has a positive semidefinite stress matrix $\bar{\boldsymbol{\Omega}}$ satisfying $\text{rank}(\bar{\boldsymbol{\Omega}}) = n - d - 1$.

Conjecture 3. The nominal formation $(G, \boldsymbol{r})$ is affinely localizable by the leaders.

Based on the above definition, a useful lemma is given below.

Lemma 1. *[4] If Conjecture 1–3 hold, then*
1) $\bar{\boldsymbol{\Omega}}_{ff}$ is positive definite.
2) For any $\boldsymbol{p} = \left[\boldsymbol{p}_l^T, \boldsymbol{p}_f^T\right]^T \in \boldsymbol{A}(\boldsymbol{r})$, $\boldsymbol{p}_f$ can be uniquely calculated as

$$\boldsymbol{q}_f = -\bar{\boldsymbol{\Omega}}_{ff}^{-1} \bar{\boldsymbol{\Omega}}_{fl} \boldsymbol{q}_l \tag{11}$$

Therefore, the shape of the formation can be obtained via only controlling the leaders.

2.3 Modeling

In this paper, the model of UAVs can be considered as the second-order dynamical model, which can be expressed as

$$\begin{cases} \dot{\boldsymbol{q}}_i = \boldsymbol{p}_i \\ \dot{\boldsymbol{p}}_i = \boldsymbol{u}_i \end{cases} \tag{12}$$

For UAV α_i in the formation, its neighbor set is

$$N_i = \left\{ \alpha_i \mid \left\| \boldsymbol{q}_i - \boldsymbol{q}_j \right\| < \boldsymbol{d}_{ij}, (i, j = 1, 2, ..., n)(i \neq j) \right\} \tag{13}$$

where any two UAVs are considered neighbors to each other when the distance between them is less than $\boldsymbol{d}_{ij}$.

In addition, in order to the UAVs to avoid obstacles, the repulsion field function is introduced as

$$U_o\left(\|\boldsymbol{d}_{i,o_n}\|\right) = \frac{k}{2}\bar{G}\left(\|\boldsymbol{d}_{i,o_n}\| - \boldsymbol{L}_o\right)^2 \tag{14}$$

where, $\bar{G}$ is the gravitational constant; k is the obstacle avoidance control coefficient; $\boldsymbol{d}_{i,o_n}$=$\boldsymbol{q}_{o_n}$-$\boldsymbol{q}_i$ is the distance between UAV α_i and the Nth obstacle detected by the α_i ($\boldsymbol{q}_{o_n}$ is the position of the Nth obstacle detected by α_i, $N = 1, 2, ..., N'$ where N' is the total number of obstacles detected by the α_i).

3 Obstacle Avoidance Control of UAVs

In this section, we design the control law for UAVs to avoid obstacle based on the affine formation.

3.1 Control law design

For the formation to reach the destination successfully, conjecture 4 is given as follows.

Conjecture 4. The leaders in the formation can obtain some information including the flight target of the formation, route planning information, formation change instructions, etc. issued by the ground station in real time through the wireless transmission of signals, and the corresponding flight actions will be made by the leaders in time.

Based on Conjecture 4, the target formation can be formed when the follower can track the leader accurately. The position tracking error of the followers is defined as

$$\boldsymbol{\delta}_{qf}(t) = \boldsymbol{q}_f(t) - \boldsymbol{q}_f^*(t) = \boldsymbol{q}_f(t) + \bar{\boldsymbol{\Omega}}_{ff}^{-1}\bar{\boldsymbol{\Omega}}_{fl}\boldsymbol{q}_l^*(t) \tag{15}$$

And the speed tracking error is

$$\boldsymbol{\delta}_{pf}(t) = \boldsymbol{p}_f(t) - \boldsymbol{p}_f^*(t) = \boldsymbol{p}_f(t) + \bar{\boldsymbol{\Omega}}_{ff}^{-1}\bar{\boldsymbol{\Omega}}_{fl}\boldsymbol{p}_l^*(t) \tag{16}$$

In this way, the control objective is to design the control algorithm for the followers to guarantee $\boldsymbol{\delta}_{pf}(t)\rightarrow 0$ and $\boldsymbol{\delta}_{qf}(t)\rightarrow 0$ when $t\rightarrow\infty$.

It can be seen that the stress matrix and $\boldsymbol{M}$ matrix have the same dimension and structure based on the definitions in Eqs. (8)-(10), then we can define

$$\bar{\boldsymbol{\Omega}}' = \bar{\boldsymbol{L}} \odot \bar{\boldsymbol{\Omega}} = \begin{bmatrix} \bar{\boldsymbol{\Omega}}'_{ll} & \bar{\boldsymbol{\Omega}}'_{lf} \\ \bar{\boldsymbol{\Omega}}'_{fl} & \bar{\boldsymbol{\Omega}}'_{ff} \end{bmatrix} \tag{17}$$

where $\bar{\boldsymbol{\Omega}}'_{ff}$ is a symmetric positive definite and nonsingular matrix. According to the properties of the $\boldsymbol{M}$ matrix and stress matrix, $\bar{\boldsymbol{\Omega}}'$ can be used as a communication matrix with variable weight control gain. Here, the original communication mode is not be affected with the weight changes.

At this point, the Follower control laws are obtained as

$$\begin{aligned} \dot{\boldsymbol{p}}_i = & -\frac{1}{\gamma_i} \sum_{j \in N_i} w'_{ij} \left[\left(\boldsymbol{q}_i - \boldsymbol{p}_j \right) + k_p \left(\boldsymbol{p}_i - \boldsymbol{p}_j \right) - \dot{\boldsymbol{p}}_j \right] \\ & - \frac{k}{\gamma_i} \boldsymbol{p}_i \left[\sum_{N=1}^{N'} \bigtriangledown U_o \left(\| \boldsymbol{d}_{i,o_n} \| \right) \right] \end{aligned} \tag{18}$$

where, $\gamma_i = \sum\limits_{j \in N_i} w'_{ij}$; k_p is the control coefficient greater than 0.

3.2 Analysis of system stability

Theorem 1. *Consider a formation system composed of n UAVs with the characteristics of Eq. (12). If Conjectures 1 to 4 hold, under the control law of Eq. (18), the followers can affinely converge to the desired formation without collisions occurring between the ith UAV and other UAVs during their flying process.*

Proof. Multiplying γ_i on both sides of the control law in Eq. (18) yields

$$\begin{aligned} \sum_{j \in N_i} w'_{ij} \left(\dot{\boldsymbol{p}}_i - \dot{\boldsymbol{p}}_j \right) = & \sum_{j \in N_i} w'_{ij} \left[\left(\boldsymbol{q}_i - \boldsymbol{p}_j \right) + k_p \left(\boldsymbol{p}_i - \boldsymbol{p}_j \right) \right] \\ & - \boldsymbol{p}_i k \left[\sum_{N=1}^{N'} \bigtriangledown U_o \left(\| \boldsymbol{d}_{i,o_n} \| \right) \right] \end{aligned} \tag{19}$$

The matrix form of Eq. (19) is

$$\begin{aligned} \bar{\boldsymbol{\Omega}}'_{ff} \dot{\boldsymbol{p}}_f + \bar{\boldsymbol{\Omega}}'_{fl} \dot{\boldsymbol{p}}_l^* = & - \left(\bar{\boldsymbol{\Omega}}'_{ff} \boldsymbol{q}_f + \bar{\boldsymbol{\Omega}}'_{fl} \boldsymbol{q}_l^* \right) \\ & - k_p \left(\bar{\boldsymbol{\Omega}}'_{ff} \boldsymbol{p}_f + \bar{\boldsymbol{\Omega}}'_{fl} \boldsymbol{p}_l^* \right) \\ & - \boldsymbol{p}_i k \left[\sum_{N=1}^{N'} \bigtriangledown U_o \left(\| \boldsymbol{d}_{i,o_n} \| \right) \right] \end{aligned} \tag{20}$$

Then, we can obtain

$$\begin{aligned} \dot{\boldsymbol{p}}_f = & - \left(\bar{\boldsymbol{\Omega}}'_{ff} \bar{\boldsymbol{\Omega}}'^{-1}_{ff} \boldsymbol{q}_f + \bar{\boldsymbol{\Omega}}'_{fl} \bar{\boldsymbol{\Omega}}'^{-1}_{ff} \boldsymbol{q}_l^* \right) \\ & - k_p \left(\bar{\boldsymbol{\Omega}}'_{ff} \bar{\boldsymbol{\Omega}}'^{-1}_{ff} \boldsymbol{p}_f + \bar{\boldsymbol{\Omega}}'_{fl} \bar{\boldsymbol{\Omega}}'^{-1}_{ff} \boldsymbol{p}_l^* \right) \\ & - \boldsymbol{p}_i \bar{\boldsymbol{\Omega}}'^{-1}_{ff} k \left[\sum_{N=1}^{N'} \bigtriangledown U_o \left(\| \boldsymbol{d}_{i,o_n} \| \right) \right] - \bar{\boldsymbol{\Omega}}'^{-1}_{ff} \bar{\boldsymbol{\Omega}}'_{fl} \dot{\boldsymbol{p}}_l^* \\ = & - \boldsymbol{\delta}_{qf} - k_p \boldsymbol{\delta}_{pf} - \bar{\boldsymbol{\Omega}}'^{-1}_{ff} \bar{\boldsymbol{\Omega}}'_{fl} \dot{\boldsymbol{p}}_l^* \\ & - \boldsymbol{p}_i \bar{\boldsymbol{\Omega}}'^{-1}_{ff} k \left[\sum_{N=1}^{N'} \bigtriangledown U_o \left(\| \boldsymbol{d}_{i,o_n} \| \right) \right] \end{aligned} \tag{21}$$

Furthermore, taking the differential with respect to time t on both sides of Eq. (16) and substituting Eq. (21) into it, we have

$$\begin{aligned}\dot{\boldsymbol{\delta}}_{pf} =&\dot{\boldsymbol{p}}_f(t) + \bar{\boldsymbol{\Omega}}'^{-1}_{ff}\bar{\boldsymbol{\Omega}}'_{fl}\boldsymbol{p}_l^* \\ =&\boldsymbol{\delta}_{qf} - k_p\boldsymbol{\delta}_{pf} - \boldsymbol{p}_i\bar{\boldsymbol{\Omega}}'^{-1}_{ff}k\left[\sum_{N=1}^{N'} \triangledown U_o\left(\|\boldsymbol{d}_{i,o_n}\|\right)\right]\end{aligned} \tag{22}$$

To show the system stability of the formation, the candidate Lyapunov function is set as

$$V = \frac{1}{2}\boldsymbol{\delta}_{qf}^T\bar{\boldsymbol{\Omega}}'_{ff}\boldsymbol{\delta}_{qf} + V_o + \frac{1}{2}\boldsymbol{\delta}_{pf}^T\bar{\boldsymbol{\Omega}}'_{ff}\boldsymbol{\delta}_{pf} \tag{23}$$

where,

$$V_o = \frac{k'}{2}\bar{G}\left[\sum_{N=1}^{N'}\left(\|\boldsymbol{d}_{i,o_n}\| - \boldsymbol{L}_o\right)^2\right] \tag{24}$$

and $k' = k \cdot \boldsymbol{\delta}_{qf}$.

Taking the time derivative of the candidate Lyapunov function V as

$$\begin{aligned}\dot{V} =&\boldsymbol{\delta}_{qf}^T\bar{\boldsymbol{\Omega}}'_{ff}\dot{\boldsymbol{\delta}}_{qf} + \dot{V}_o + \boldsymbol{\delta}_{pf}^T\bar{\boldsymbol{\Omega}}'_{ff}\dot{\boldsymbol{\delta}}_{pf} \\ =&\boldsymbol{\delta}_{qf}^T\bar{\boldsymbol{\Omega}}'_{ff}\boldsymbol{\delta}_{pf} + \dot{\boldsymbol{q}}_i k'\triangledown U_o\left(\|\boldsymbol{d}_{i,o_n}\|\right) \\ &+ \boldsymbol{\delta}_{pf}^T\bar{\boldsymbol{\Omega}}'_{ff}\left\{\boldsymbol{\delta}_{qf} - k_p\boldsymbol{\delta}_{pf} - \bar{U}_o\right\} \\ =&k_p\boldsymbol{\delta}_{pf}^T\bar{\boldsymbol{\Omega}}'_{ff}\boldsymbol{\delta}_{pf} < 0\end{aligned} \tag{25}$$

where

$$\bar{U}_o = \boldsymbol{p}_i\bar{\boldsymbol{\Omega}}'^{-1}_{ff}k\left[\sum_{N=1}^{N'} \triangledown U_o\left(\|\boldsymbol{d}_{i,o_n}\|\right)\right] \tag{26}$$

Since $\dot{V} < 0$, V is non-increasing and bounded. Therefore, V converges as $t \to \infty$. At this time, the followers in the formation form the desired formation, and the followers have the ability to avoid obstacles and will not collide with each other. This completes the proof.

4 Prescribed Convergence Time Control

The problem on stable convergence within the prescribed time of the UAVs formation is studied in this section.

4.1 Prescribed convergence time

To ensure the efficiency of formation transformation, the predetermined time convergence theory is introduced, which can preset the convergence time of the affine transformation. The control input of the formation system can be expressed as

$$\boldsymbol{u} = (\boldsymbol{u}_1, \boldsymbol{u}_2, ..., \boldsymbol{u}_l, \boldsymbol{u}_{l+1}, ..., \boldsymbol{u}_n) \tag{27}$$

where T is time for formation flight. Combining with Eq. (3), the formation system can be described as

$$\dot{\boldsymbol{q}} = \boldsymbol{f}(\boldsymbol{q}(t), \boldsymbol{u}(t), t) \tag{28}$$

Here, the initial state of the system is assumed as $\boldsymbol{q}(t_0)$=$\boldsymbol{q}_0$. Considering that the functions in equation Eq. (28) are all nonlinear, which means the model of the formation system is a nonlinear time-varying system. To realize the predetermined time convergence control of the system, the state equation of Eq. (28) will be linearized in the following.

The nonlinear function in Eq. (28) is expanded into a Taylor series in the field of the operating point $(\boldsymbol{q}_0, \boldsymbol{u}_0, t)$, which the terms of the quadratic and the higher orders than 2 are omitted. In this case, the following equality holds

$$\begin{aligned} \boldsymbol{f}(\boldsymbol{q}, \boldsymbol{u}, t) =& \boldsymbol{f}(\boldsymbol{q}_0, \boldsymbol{u}_0, t) + \frac{\partial \boldsymbol{f}}{\partial \boldsymbol{q}^T} \mid_{\boldsymbol{q}_0, \boldsymbol{u}_0, t} \cdot \Delta \boldsymbol{q} \\ &+ \frac{\partial \boldsymbol{f}}{\partial \boldsymbol{u}^T} \mid_{\boldsymbol{q}_0, \boldsymbol{u}_0, t} \cdot \Delta \boldsymbol{u} \end{aligned} \tag{29}$$

where, $\Delta\boldsymbol{q}$=$\boldsymbol{q}$-$\boldsymbol{q}_0$, $\Delta\boldsymbol{u}$=$\boldsymbol{u}$-$\boldsymbol{u}_0$. Then, we have

$$\dot{\boldsymbol{q}} = \dot{\boldsymbol{q}}_0 + \Delta \dot{\boldsymbol{q}} \tag{30}$$

The following formula is satisfied at the working point

$$\dot{\boldsymbol{q}}_0 = \boldsymbol{f}(\boldsymbol{q}_0, \boldsymbol{u}_0, t) \tag{31}$$

Therefore, the state space equation linearized by small perturbation can be calculated as

$$\begin{aligned} \Delta \dot{\boldsymbol{q}} =& \frac{\partial \boldsymbol{f}}{\partial \boldsymbol{q}^T} \mid_{\boldsymbol{q}_0, \boldsymbol{u}_0} \cdot \Delta \boldsymbol{q} + \frac{\partial \boldsymbol{f}}{\partial \boldsymbol{u}^T} \mid_{\boldsymbol{q}_0, \boldsymbol{u}_0} \cdot \Delta \boldsymbol{u} \\ =& \boldsymbol{A}(t) \Delta \boldsymbol{q} + \boldsymbol{B}(t) \Delta \boldsymbol{u} \end{aligned} \tag{32}$$

where,

$$\boldsymbol{A}(t) = \frac{\partial \boldsymbol{f}}{\partial \boldsymbol{q}^T} \mid_{\boldsymbol{q}_0, \boldsymbol{u}_0} = \begin{bmatrix} \frac{\partial \boldsymbol{f}_1}{\partial \boldsymbol{q}_1} & \cdots & \frac{\partial \boldsymbol{f}_1}{\partial \boldsymbol{q}_n} \\ \vdots & \ddots & \vdots \\ \frac{\partial \boldsymbol{f}_n}{\partial \boldsymbol{q}_1} & \cdots & \frac{\partial \boldsymbol{f}_n}{\partial \boldsymbol{q}_n} \end{bmatrix}_{\boldsymbol{q}_0, \boldsymbol{u}_0, t} \tag{33}$$

$$\boldsymbol{B}(t) = \frac{\partial \boldsymbol{f}}{\partial \boldsymbol{u}^T} \mid_{\boldsymbol{q}_0, \boldsymbol{u}_0} = \begin{bmatrix} \frac{\partial \boldsymbol{f}_1}{\partial \boldsymbol{u}_1} & \cdots & \frac{\partial \boldsymbol{f}_1}{\partial \boldsymbol{u}_n} \\ \vdots & \ddots & \vdots \\ \frac{\partial \boldsymbol{f}_n}{\partial \boldsymbol{u}_1} & \cdots & \frac{\partial \boldsymbol{f}_n}{\partial \boldsymbol{u}_n} \end{bmatrix}_{\boldsymbol{q}_0, \boldsymbol{u}_0, t} \tag{34}$$

In this way, the linear system shown in Eq. (32) can replace the nonlinear system in Eq. (28) with sufficient accuracy, when the nonlinear system moves near the operating point.

It can be known from Theorem 1 that the formation system in Eq. (32) is stable and asymptotically convergent in the time domain space of t, that is, when $t \to \infty$, then $\Delta \boldsymbol{q}(t) \to 0$, and the system forms a standard configuration. To achieve predetermined time convergence, the time t is transformed and the ρ-domain space is introduced.

Suppose there exists a time-varying scaling function

$$a(t) = \frac{a_0 t}{1 - \frac{t}{T_1}} \tag{35}$$

where, T_1 is the predetermined convergence time; a_0 is a constant greater than 0. Taking the derivative of time t on both sides of Eq. (35), we get

$$a'(t) = \frac{a_0}{\left(1 - \frac{t}{T_1}\right)^2} := \alpha(\rho) \tag{36}$$

Let $\rho = a(t)$, and we have $t = a^{-1}(\rho)$ ($a^{-1}(t)$ existed) and $d\rho = a'(t)dt$, which can be further written as

$$\frac{dt}{d\rho} = \frac{1}{a'(t)} = \frac{1}{\alpha(\rho)} \tag{37}$$

Since t and ρ have the following transformation relationship

$$t = \frac{\rho}{a_0 + \frac{\rho}{T_1}} \tag{38}$$

and combining Eq. (36), the expression of $\alpha(\rho)$ can be rewritten as

$$\alpha(\rho) = \frac{da}{dt} = \frac{a_0}{\left(1 - \frac{t}{T_1}\right)^2} = \frac{a_0}{\left(1 - \frac{\rho}{a_0 T_1 + \rho}\right)^2} \geq 0 \tag{39}$$

It can be seen form Eq. (39), when $t \in [0, \infty)$, then $\rho \in [0, T_1]$. Converting the formation system in Eq. (32) to the ρ-domain, we have

$$\begin{aligned} \Delta \dot{\boldsymbol{q}}(\rho) =& \frac{d\Delta \boldsymbol{q}}{d\rho} = \frac{d\Delta \boldsymbol{q}}{dt} \cdot \frac{dt}{d\rho} \\ =& \frac{1}{\alpha(\rho)} \left[\boldsymbol{A}(\rho)\Delta \boldsymbol{q} + \boldsymbol{B}(\rho)\Delta \boldsymbol{u}\right] \end{aligned} \tag{40}$$

From Eq. (40), the $\Delta \dot{\boldsymbol{q}}(\rho)$ can be obtained. Further, the control input $\Delta \boldsymbol{u}(\rho)$ in the ρ-domain can be calculated, which can make the system asymptotically converge under the ρ-domain. Then, the new control input $\Delta \bar{\boldsymbol{u}}(t)$ under the t-domain can be obtained through the conversion relationship in Eq. (38). It follows that the new control input matrix of the system $\boldsymbol{u}'$ can be obtained.

At this time, for the formation system, when $t = 0$ then $\rho = 0$; when $t = T_1$ then $\rho = \infty$. That is, the system will converge asymptotically when $\rho \to \infty$ under the ρ-domain; and the system converges asymptotically under the t-domain when $t \to T_1$ under the t-domain.

4.2 Analysis of system stability

Based on the analysis in the previous section , the following theorem can be obtained.

Theorem 2. *Consider a formation system composed of n UAVs with the characteristics of Eq. (12). The start time is $t_0 = 0s$ and the end time is $t_e = T_1 s$. If Conjectures 1 to 4 hold, under the new control law of $\boldsymbol{u}'$, the followers can affinely converge to the desired formation at time T_1 without collisions occurring between the ith UAV and other UAVs during their flying process.*

Proof. To prove that the formation system can form the desired formation at time T_1, that is, to prove the state tracking error can converge to zero asymptotically in the ρ-domain.

At this time, the Lyapunov function of Eq. (23) is still be selected. Then, differentiating both sides of Eq. (23) with respect to the variable ρ yields

$$\frac{dV}{d\rho} = \frac{dV}{dt} \cdot \frac{dt}{d\rho} = \frac{dV}{dt} \cdot \frac{1}{\alpha(\rho)} \tag{41}$$

It follows from Eq. (25) that $\frac{dV}{dt} < 0$, and $\frac{1}{\alpha(\rho)} > 0$ based on the result of Eq. (39). Therefore, we have $\frac{dV}{d\rho} < 0$.

That is, the stability of the system converges asymptotically, which means the above-mentioned time domain transformation does not affect the original stability of the system. This completes the proof.

5 Numerical Simulation

In this section, numerical simulations were presented to demonstrate the validity of the control law used in the paper.

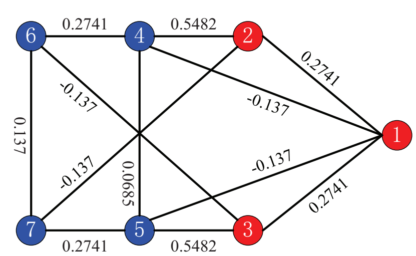

Fig. 1: The nominal formation for the simulation.

The nominal formation $(G, \boldsymbol{r})$ of 7 UAVs for the simulation is shown in Fig. 1, in which the first three UAVs are denoted as leaders and the rest UAVs are followers. Here, the weight of the stress matrix is the same as the Zhao [4], which can be proved that conjecture 1-3 hold.

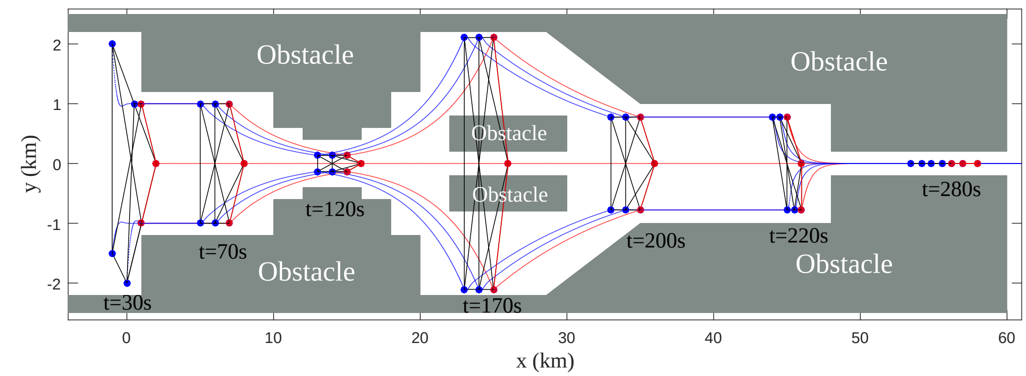

Fig. 2: Trajectories of UAVs affine formation obstacle avoidance.

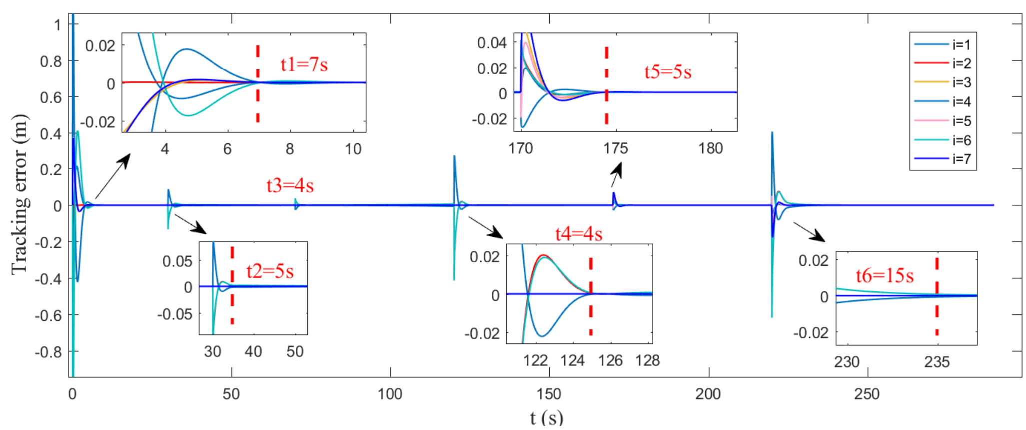

Fig. 3: Tracking error of formation system.

In Fig. 2, the 7 UAVs form the nominal formation successfully at time 70s. To through the obstacle zone, the corresponding translation, rotation and s-caling actions are made by the formation at time 120s, 170s, 200s, 220s, 280s, respectively. Fig. 3 are the tracking error curves, which are the errors between the UAVs and their corresponding desired position. There are 6 transformations in the whole process. Taking into account factors such as flight distance and mission, each action is set in turn to be executed within 7s, 5s, 4s, 4s, 5s, and 15s. It can be observed from Fig. 3 that the UAVs can converge to zero within the prescribed time.

The simulation results demonstrate the formation has high maneuverability of changing the shape to avoid obstacles, which indicates that the proposed formation control law has good performance.

6 Conclusion

In this paper, the affine formation obstacle avoidance control method of UAVs with prescribed convergence time has been presented. First, the control law for the formation according to the improved affine formation has been proposed, which will be more conducive to practical application. Then, the control of prescribed convergence time is introduced to recalculate the control law based on ρ-domain, which can preset the time of forming desired configuration. Finally, the simulation results have shown the effectiveness of the proposed control approach.

References

1. Hu, J.W., Wang, M., Zhao, C.H., Pan, Q., Du, C.: Formation control and collision avoidance for multi-UAV systems based on Voronoi partition. Sci. China Technol. Sci. 63, 65–72 (2020). https://doi.org/10.1007/s11431-018-9449-9.
2. Wu, Y., Gou, J., Hu, X., Huang, Y.: A new consensus theory-based method for formation control and obstacle avoidance of UAVs. Aerosp. Sci. Technol. 107, (2020). https://doi.org/10.1016/j.ast.2020.106332.
3. Ge, M., Cao, D., Zhao, Z.: Design and Implementation of UAV Formation Controller. In: Yan, L., Duan, H., Yu, X. (eds) Advances in Guidance, Navigation and Control. Lecture Notes in Electrical Engineering, vol 644. Springer, Singapore, (2022). https://doi.org/10.1007/978-981-15-8155-7_306.
4. Zhao, S.: Affine Formation Maneuver Control of Multiagent Systems. IEEE Trans. Automat. Contr. 63, 4140–4155 (2018). https://doi.org/10.1016/j.ifacol.2020.12.2540.
5. Luo, Z., Zhang, P., Ding, X., Tang, Z., Wang, C., Wang, J.: Adaptive Affine Formation Maneuver Control of Second-Order Multi-Agent Systems with Disturbances. 16th IEEE Int. Conf. Control. Autom. Robot. Vision, ICARCV 2020. 1071–1076 (2020). https://doi.org/10.1109/ICARCV50220.2020.9305372.
6. Zhi, H., Chen, L., Li, C., Guo, Y.: Leader-Follower Affine Formation Control of Second-Order Nonlinear Uncertain Multi-Agent Systems. IEEE Trans. Circuits Syst. II Express Briefs. 68, 3547–3551 (2021). https://doi.org/10.1109/TCSII.2021.3072652.
7. Chen, L., Mei, J., Li, C., Ma, G.: Distributed Leader-Follower Affine Formation Maneuver Control for High-Order Multiagent Systems. IEEE Trans. Automat. Contr. 65, 4941–4948 (2020). https://doi.org/10.1109/TAC.2020.2986684.
8. Xu, Y., Lin, Z., Zhao, S.: Distributed Affine Formation Tracking Control of Multiple Fixed-Wing UAVs. Chinese Control Conf. CCC. 2020-July, 4712–4717 (2020). https://doi.org/10.23919/CCC50068.2020.9188925.
9. Wang, J., Ding, X., Wang, C., Liang, L., Hu, H.: Affine formation control for multi-agent systems with prescribed convergence time. J. Franklin Inst. 358, 7055–7072 (2021). https://doi.org/10.1016/j.jfranklin.2021.07.019.
10. Trinh, M.H., Ahn, H.S.: Finite-Time Bearing-Based Maneuver of Acyclic Leader-Follower Formations. IEEE Control Syst. Lett. 6, 1004–1009 (2022). https://doi.org/10.1109/LCSYS.2021.3088299.
11. Wang, J., Ding, X., Wang, C., Liang, L., Hu, H.: Affine formation control for multi-agent systems with prescribed convergence time. J. Franklin Inst. 358, 7055–7072 (2021). https://doi.org/10.1016/j.jfranklin.2021.07.019.